CORE
Metadata, citation and similar papers at core.ac.uk

東北大学機関リポジトリ
TOUR
Tohoku University Repository

Manipulation and Observation of Carbon Nanotubes in Water Under an Optical Microscope Using a Microfluidic Chip

著者	山西　陽子
journal or publication title	IEEE Transactions on Nanotechnology
volume	8
number	4
page range	463-468
year	2009
URL	http://hdl.handle.net/10097/46536

doi: 10.1109/TNANO.2008.2012346

Manipulation and Observation of Carbon Nanotubes in Water Under an Optical Microscope Using a Microfluidic Chip

Naoki Inomata, *Student Member, IEEE*, Yoko Yamanishi, *Member, IEEE*, and Fumihito Arai, *Member, IEEE*

***Abstract*—We successfully manipulated and observed carbon nanotubes (CNTs) in water, under an optical microscope. We employed a quenching observation method, where the intensity of fluorescent reagents around CNTs is decreased due to energy transfer. By this method, CNTs can be observed continuously for a long time by adding a new fluorescent reagent after fluorescence photobleaching. However, we must adjust the density of the fluorescent reagent around CNTs, which is extremely difficult to control. Thus, we built a fluorescent reagent supply system in a microfluidic chip. We found that polydimethylsiloxane with a porous structure could absorb the fluorescent reagent as a carrier and supply the reagent at a high and constant density for a long time. In experiments, using a microstirrer, we mixed two fluids uniformly, and succeeded in controlling the density of the fluorescent reagent. In addition, we applied dielectrophoretic (DEP) force for trapping the CNTs. The electrode material was indium–tin oxide, which is suitable for manipulation and observation of CNTs under an optical microscope because of its high conductive properties and good transparency. In these experiments, we trapped CNTs by DEP and observed CNTs by quenching on the chip, and confirmed that the fluorescent image of the CNTs was clearer than their bright-field images.**

***Index Terms*—Carbon nanotubes (CNTs), fluorescent image, microchannel, microfabrication.**

I. Introduction

CARBON nanotubes (CNTs) have attracted attention as a new nanomaterial because of their novel structure and mechanical and electric characteristics [1]. In the field of biotechnology, the requirements for using nanodevices have increased in recent years. Research into the fabrication of nanodevices, such as sensors or transistor elements, is performed by manipulating individual CNTs with an atomic force microscope and an electron microscope [2], [3]. However, the CNTs and devices for manipulating them must be placed in a vacuum environment to manipulate and observe them with a typical electron microscope [2], [3], and moreover, the surface of CNTs is damaged by the irradiation of the electron beam.

Therefore, real-time observation and operation of CNTs in solutions must be carried out under optical microscopes. To achieve this, it is necessary to disperse CNTs in a solvent to form a stable solution, and then, observe them in this solution. There are several methods for dispersing CNTs, such as a surface structural change [4] and surface coating with a surface-active agent [5].

Also, the representative examples of a major visualization method are fluorescent observation [6], Raman scattering observation [7]–[9], photoluminescence observation [10], [11], and those that have been used in biotechnology field recently [12], [13]. However, the fluorescent observation has a problem of very short observation time. Moreover, it is impossible to observe the discolored CNT sample, because the fluorescent reagent is physically adsorbed on the surface of the CNTs. Raman scattering observation has a problem of low sensitivity and is affected by the background noise due to the scattering light, which is caused by fine particles, etc., around the subject. In the case of photoluminescence observation, we can observe only semiconductive CNTs, not all sort of CNTs can be applied to be observed.

In this paper, we examined the quenching phenomenon as a way of observing CNTs in solution. The quenching phenomenon has been used to observe CNTs successfully [14], [15]. This method makes long-term and repetitive observations of CNTs feasible simply by adding a fluorescent reagent [15]. Also, this method is not invasive to the CNT surface and appropriate for nonintrusive measurement such as electron microscope. Also, it is important to note that this method is effective for continuous observation in solution. Moreover, they are economical because we can observe easily by using a fluorescent microscope. However, it is necessary to adjust the density of the fluorescent reagent around the CNTs precisely, and this is extremely difficult to control because the appropriate density depends on the density of the CNTs dispersed in the solution. Therefore, we propose a novel system for supplying the fluorescent reagent.

On the other hand, dielectrophoresis (DEP) [16], [17], optical tweezers [14], and focused laser beam [9] have been used frequently as a CNT manipulation method in the aqueous fluid. While it is difficult to manipulate specific CNT with DEP, the optical tweezers or the focused laser beam has advantage of assembling specific CNT on the device. However, these methods are not always effective manipulation method because of their low manipulation performances. The greatest characteristic of DEP we employed in this paper is large-scale assembly, and

Manuscript received August 12, 2008; revised December 11, 2008. First published January 13, 2009; current version published July 9, 2009. This work was supported in part by the Core Research for Evolutional Science and Technology (CREST), in part by the Japan Science and Technology (JST), in part by the Research and Development Program for New Bioindustry Initiatives, and in part by the Ministry of Education, Culture, Sports, Science and Technology under Grant 17040017. The review of this paper was arranged by Editor B. Nelson.

The authors are with the Department of Bioengineering and Robotics, Tohoku University, Sendai 980-8579, Japan (e-mail: inomata@imech.mech.tohoku.ac.jp; yoko@imech.mech.tohoku.ac.jp; arai@imech.mech.tohoku.ac.jp).

Color versions of one or more of the figures in this paper are available online at http://ieeexplore.ieee.org.

Digital Object Identifier 10.1109/TNANO.2008.2012346

1536-125X/$25.00 © 2009 IEEE

Authorized licensed use limited to: TOHOKU UNIVERSITY. Downloaded on March 10,2010 at 00:14:00 EST from IEEE Xplore. Restrictions apply.

many studies are reported on the applied DEP with assembling techniques [18], [19]. The electrode material was indium–tin oxide (ITO), which is suitable for manipulation and observation of CNTs under an optical microscope because of its high conductive properties and good transparency. In these experiments, we trapped CNTs by DEP and observed CNTs by quenching on the chip, and confirmed that the fluorescent image of the CNTs was clearer than their bright-field images. For this study, we successfully manipulated the system and confirmed that CNTs can be observed more clearly by using the quenching phenomenon.

II. Design of the Microfluidic Chip

We used a polymer-based porous structure that can adsorb a fluorescent reagent as a carrier to supply the fluorescent reagent. We used a microfluidic chip with an on-chip microtool to mix the fluids uniformly. One fluid flow includes a fluorescent reagent and the other does not. The microtool for these experiments was microfabricated with photolithography techniques used for mass production. Typically, actuators utilizing electrostatic power and optical pressure are used to drive small objects. Compared to these, actuators utilizing magnetic force are stronger and can provide large displacements. Magnetic actuators also have the advantage of being harmless to living things. Therefore, magnetically driven valves and pumps are used extensively in such research [20], [21]. However, disposable and flexible molded actuators are rare. Therefore, we used a magnetically driven microtool that is fabricated by molding a polymer containing magnetic particles [22]. DEP force is used to trap CNTs in microchannels [23], and it was observed that they were caught in the electrode gap in this study.

Polydimethylsiloxane (PDMS) was used as the polymer structural material supplying the fluorescent reagent. We report the observation of CNTs while using the system to supply the fluorescent reagent at a specific density. We adjusted the density of the fluorescent reagent by controlling the flow rate of deionized (DI) water in the two inlets; the magnetically driven microtool kept the density in microchannel uniform. Fig. 1 shows the chip design, which we fabricated using photolithography and soft lithography techniques. The chip structure consists mainly of the reagent supply module and the CNT observation module.

The reagent supply module consists of a microchannel, a magnetically driven microtool, and a porous PDMS carrier. Two inlet ports are mounted, and the porous PDMS carrier, which is soaked in a fluorescent reagent, is set in the path of one channel. Fluorescent reagent is extracted from this carrier when DI water passes over it. The magnetically driven microtool is set up at the confluence point of these two passages, and mixes them to provide uniform density in the channel. Without the microtool, it is difficult to mix the two flows, and a laminar two-layer sheath flow is obtained. Therefore, the density of the fluorescent reagent is controlled in the channel. The stirrer is turned using magnets mounted on a motor placed under the chip (Fig. 5). We could adjust the density of the fluorescent reagent over a wide range by mixing the flows in the two channels.

The CNT observation module consists of ITO electrodes and a microchannel made of PDMS. ITO electrodes are suitable for manipulation and observation of CNTs under an optical microscope because ITO is highly conductive and transparent. We manipulated CNTs with the DEP force. The electrode tips forming the gap were smoothened to decrease the amount of trapped CNTs. By flowing the liquid containing dispersed CNTs into the microchannel and applying a voltage to the electrodes, we could trap the CNTs in the electrode gaps.

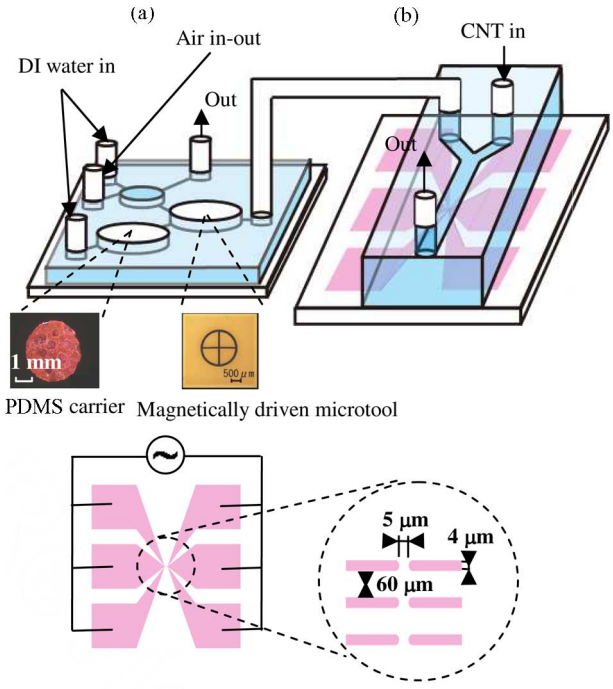

Fig. 1. Basic design of the microfluidic chip. (a) Supply module. (b) Observation module.

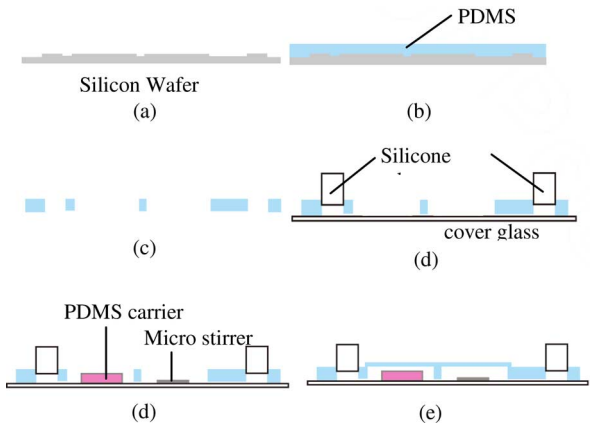

Fig. 2. Fabrication process of the reagent supply module. (a) Pattern silicon water. (b) Mold PDMS. (c) Produce a hole in PDMS mold. (d) Setup of silicone tube and cover glass; set a porous PDMS carrier and microstirrer. (e) Seal with PDMS sheet.

III. Fabrication of the Microfluidic Chip

We produced the reagent supply module according to the procedure shown in Fig. 2, based on the design shown in Fig. 1. The channels in the reagent supply module are 120 μm high and 200 μm wide. The chamber in the path of the channel and

Authorized licensed use limited to: TOHOKU UNIVERSITY. Downloaded on March 10,2010 at 00:14:00 EST from IEEE Xplore. Restrictions apply.

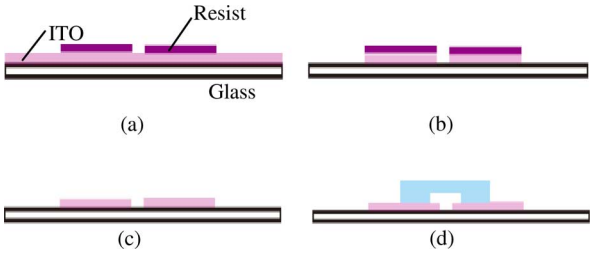

Fig. 3. Fabrication process of the observation module. (a) Patterning by photolithography. (b) After wet-etching. (c) Remove the resist. (d) Attach PDMS mold.

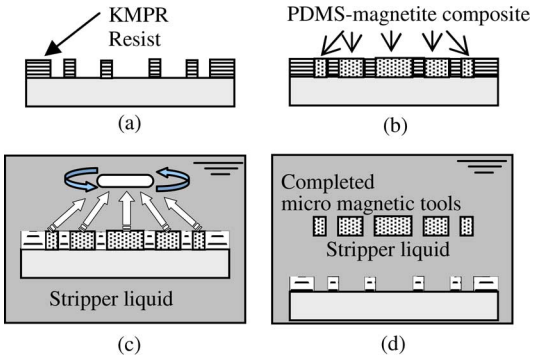

Fig. 4. Fabrication process of a micromagnetic stirrer. (a) Photolithography. (b) Molding. (c) Remove the resist. (d) Complete the tool.

at the intersection point is 5 mm in diameter. A silicon wafer was patterned, as shown in Fig. 2(a), and a 2-mm-thick layer of PDMS was molded on the wafer [Fig. 2(b)]. After the molded PDMS was removed, holes were punched at both ends of the channels of the molded PDMS to form inlets, outlets, and a chamber. The diameter of the inlets and outlets is 1.5 mm, and that of the chamber is 5 mm [Fig. 2(c)]. Next, the molded PDMS was bonded to a cover glass. A silicone tube was connected to the hole at both ends of the channels, and porous PDMS was placed in the channel. The microtool was placed in the hole at the intersection of the channels [Fig. 2(d)], and then, these holes were sealed with a thin PDMS sheet [Fig. 2(e)].

Next, we produced the CNT observation module. ITO was sputtered on the glass substrate, and an electrode pattern was deposited by photolithography [Fig. 3(a)]. ITO not covered with the electrode pattern was removed by wet etching [Fig. 3(b)], and then, the resist was removed [Fig. 3(c)] and the molded PDMS was positioned with the channels oriented, as shown in Fig. 3(d). This channel is 50 μm high and 200 μm wide.

IV. Fabrication of the Microstirrer

First, the resist was patterned on the silicon wafer [Fig. 4(a)], which is used as a mold for the magnetically driven microtool.

A mixture of PDMS and magnetic particles (50 wt%) is poured over the pattern, as shown in Fig. 4(b), and hardened at 80 °C (20 min). Finally, the patterned resist was soaked in a stripper liquid at 70 °C. To make the temperature of the stripper liquid uniform, a commercial stirrer was used [Fig. 4(c)].

The produced magnetically driven microtool has moderate flexibility (Young's modulus 5 MPa). We attached disk magnets

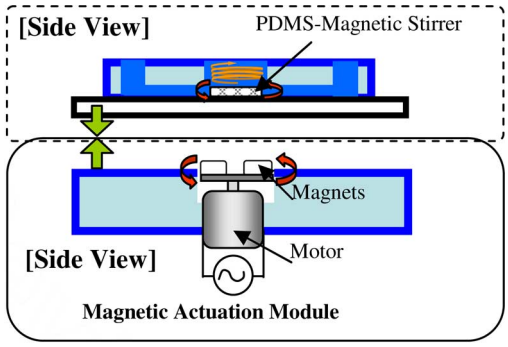

Fig. 5. Schematic view of the experimental arrangement used to produce the rotating and motion micromagnetic tool in the biochip's microchamber.

(130–550 mT) on the rotation axis of a motor, placed the motor under the chip, and rotated it. Fig. 5 shows the design of the microtool. The proposed technique can mass-produce highly accurate microtools of arbitrary shapes by photolithography; these are disposable, and it is easy to install them on a chip. This microstirrer without a center post was rotated smoothly.

V. Porous PDMS Carrier

We proposed supplying the reagent on demand using a porous PDMS carrier, and have investigated the carrier characteristics. The carrier has a porous internal structure, and is immersed in the fluorescent reagent beforehand. When porous sponge structure is soaked in a liquid, it absorbs the liquid. The liquid is easily released by applying an external force. In this case, when DI water contacts the carrier, the reagent is extracted.

We used the salt leaching method [24] to fabricate the porous PDMS carrier, because it allows control over the pore size. The pore size depends on the size of composite particles. The method is summarized as follows: first, NaCl particles (66 wt%) are mixed with PDMS before it hardens. Note that it is difficult to create a uniform density of NaCl particles when its concentration is less than 66 wt%. After mixing, it was formed into a 2-mm-thick sheet, and hardened by applying heat (80 °C). Finally, NaCl particles inside the PDMS were removed using an ultrasound bath. The produced porous PDMS sheet was punched into a 4-mm-diameter circle. The punched part was soaked in the fluorescent reagent solution for 20 h and freeze-dried for 3 h. In this experiment, two sizes of NaCl particles were used: 430 and 10–30 μm. For the reagent to penetrate deep into the carrier, it is necessary that the holes of the porous PDMS structure are connected. Fig. 6 shows images of the upper surface and the cross section of the carrier, which confirm the porous structure. To confirm that the holes are connected, we observed a section in the vicinity of the surface with a confocal microscope after the carrier was soaked in the fluorescent reagent. This sample showed fluorescent luminescence in PDMS carriers obtained with 430 and 10–30 μm pores, whereas a nonporous PDMS carrier (plain PDMS carrier) did not show such features, as shown in Fig. 7. This suggests that a PDMS carrier with a porous structure is continuous.

Authorized licensed use limited to: TOHOKU UNIVERSITY. Downloaded on March 10,2010 at 00:14:00 EST from IEEE Xplore. Restrictions apply.

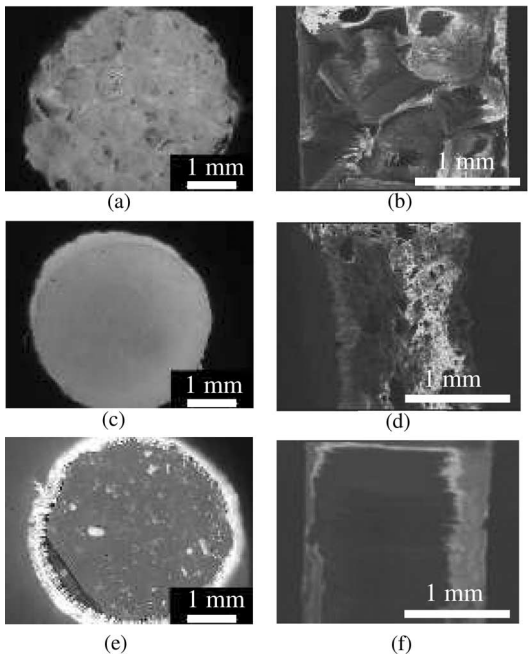

Fig. 6. (a), (c), and (e) Top and (b), (d), and (f) cross-sectional views of porous PDMS support. (a) and (b) 430 μm. (c) and (d) 10–30 μm. (e) and (f) Plane PDMS.

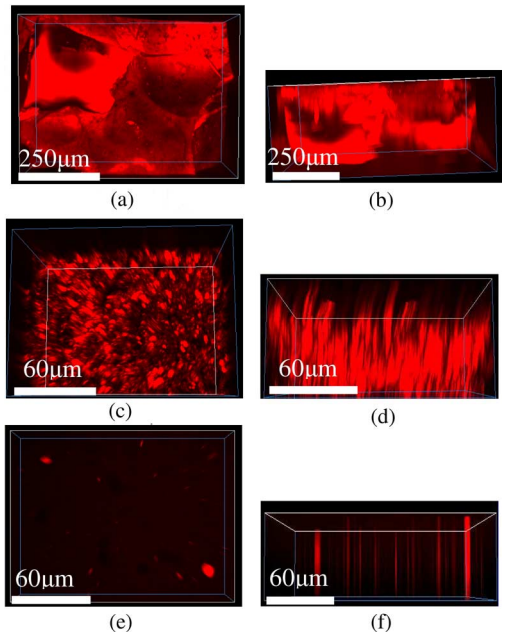

Fig. 7. (a), (c), and (e) Top images of the porous PDMS carrier and (b), (d), and (f) cross-sectional images of the porous PDMS carrier imaged by confocal laser scanning microscopy. (a) and (b) 430 μm. (c) and (d) 10–30 μm. (e) and (f) Plain PDMS.

VI. Experiment for Characterizing the Fluorescent Reagent Supply Module

We measured the fluorescent density of the fluorescent reagent solution supplied by the reagent supply module. In this experiment, we prepared three kinds of porous PDMS carriers—those obtained with 430 and 10–30 μm pores, and plain PDMS.

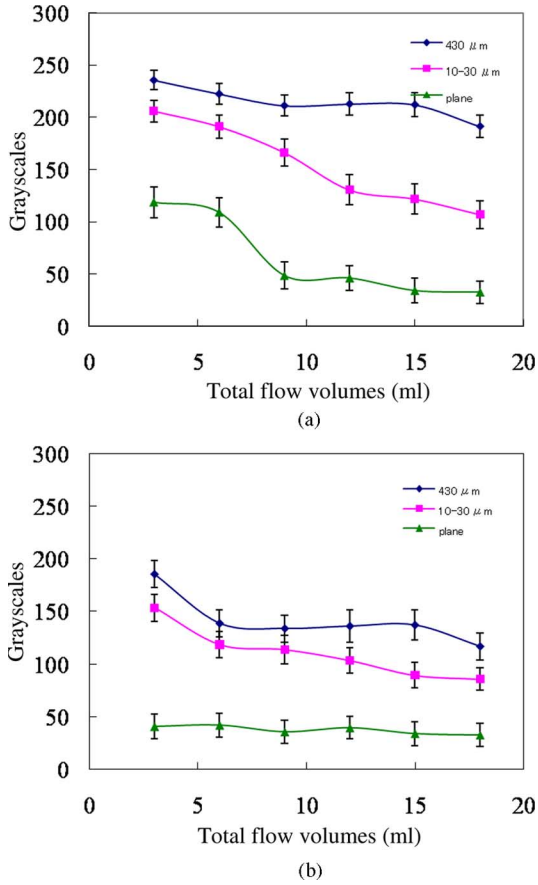

Fig. 8. Profiles of the gray scale images as a function of total flow volume. (a) 0.01 mM. (b) 0.0001 mM.

The porous PDMS was soaked in a 0.01 or 0.0001 mM fluorescent reagent solution. DI water was flowed in with a syringe pump at a velocity of 0.05 m/s for 6 min, and we observed the fluorescent solution outflow. The fluorescent intensity was quantified with a gray scale, using image analysis software (image J). Fig. 8 shows profiles of the gray scale images as a function of total flow volume for 0.01 mM reagent solution. Fig. 8 shows that the fluorescent intensity became higher as the pore size is longer. In this experiment, larger pore sizes provided higher density for longer time periods. For 0.01 mM reagent solution, the 430 μm carrier could supply a reagent in a nearly constant high density, while the density provided by the 10–30 μm carrier decreased as the flow volume increased. The plain PDMS carrier showed comparatively high density until about 5 mL, and then, the density dropped. For 0.0001 mM reagent solution, the trend is similar, although the fluorescent density was lower than that in the case of 0.01 mM. However, the plain PDMS carrier could not be used for observation of quenching phenomenon in the 0.0001 mM solution because the density was too low. This experiment demonstrated that the module could supply a constant density reagent solution using porous PDMS. The larger the pore size, the better the reagent density. However, investigation shows that too large a pore size does not work. In case of 1-mm-diameter pores, the density trend is similar to that of plain PDMS. What density is suitable depends largely on the CNT

Authorized licensed use limited to: TOHOKU UNIVERSITY. Downloaded on March 10,2010 at 00:14:00 EST from IEEE Xplore. Restrictions apply.

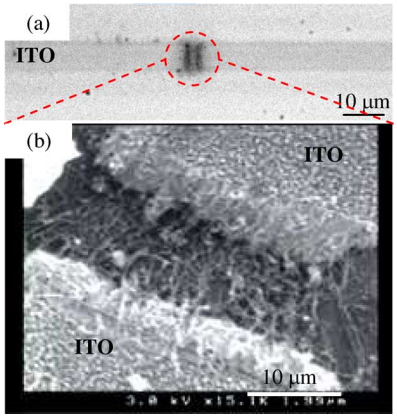

Fig. 9. (a) Scanning electron microscopy image and (b) bright-field image of CNTs attached to the ITO electrodes.

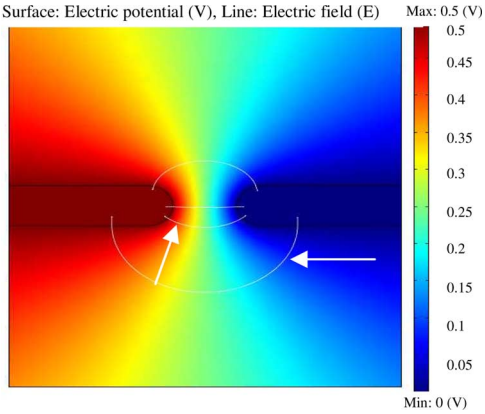

Fig. 10. Contour of the electric potential between ITO electrodes. (The arrows indicate trapped CNTs.)

density when observing the quenching phenomenon. Usually, it requires extra effort to prepare the fluorescent reagent solution in various densities. However, using the designed chip, we can fine-tune the appropriate fluorescent reagent density by simply adjusting the inflow speed of DI water. The chip is able to supply the fluorescent reagent on demand by simply setting the flow rate. Consequently, the total experimental time is shortened and efficiency is improved.

VII. Observation of CNTs

First, we confirmed that ITO electrodes can trap CNTs. The multiwall CNTs (MWNTs) used in this experiment have a purity of 95%, tube diameters of 35 nm, and tube lengths of 60–100 μm. The MWNTs were subjected to ultrasonic treatment in a 10-μM solution of 1-pyrenebutanoic acid succinimidyl ester (P130) in dimethyl sulfoxide (DMSO). It is known that CNTs agglomerate [25], but are dispersed in water if their surface is coated with P130 [26]. After this, excess P130 was removed by centrifugation (15 000 r/min, 30 min), and the CNTs were dispersed in DI water. The dispersed CNT solution was introduced to the observation chip using a syringe pump (flow velocity of 1 mL/h).

Fig. 9 shows MWNTs trapped in the vicinity of the gap with DEP force when an ac voltage is applied (0.5 V at 1 MHz). The electrode shape is different in Fig. 9 than in Fig. 1. The width is 7 μm and the gap is 3 μm. MWNTs are successfully trapped in the gap when the channel is filled with the dispersed CNT solution.

Electron microscopy images [Fig. 9(b)] clearly showed that the ITO electrodes could trap MWNTs.

In addition, we analyzed the electric field in the vicinity of the electrodes (Fig. 10). If we could predict where the CNTs would be trapped, their manipulation after trapping would be simplified.

We also used a solution with single-wall CNTs (SWNTs) dispersed in it. We successfully trapped SWNTs at the gap under experimental conditions similar to those used for the MWNTs [Fig. 11(a)]. Then, we allowed DI water to flow through the chip with the pump; eventually, fluorescence was observed after

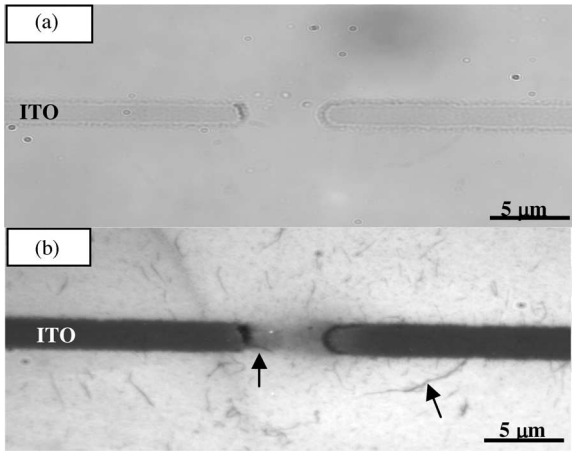

Fig. 11. Image of CNTs in water. (a) Bright-field image. (b) Fluorescent image. CNTs are attached around the ITO electrodes as predicted (indicated by the two arrows).

supplying the fluorescent reagent solution. Fig. 11 shows the bright-field and quenching images. For imaging, we used an Ar laser (488 nm, 1.4 mW) and a charge-coupled device (CCD) camera (0.3 s/frame at full resolution, 2048 $\times$ 2048 imaging array). The laser had been exposed while observation. CNTs could not be observed in the bright-field image. However, in the quenching image, CNTs can be observed clearly as dark areas. Thus, we have shown that we can observe CNTs in solution by adjusting the density of the fluorescent reagent. In addition, the CNTs were trapped as the analysis suggested (indicated by white arrows in Fig. 10 and black arrows in Fig. 11).

VIII. Conclusion

In this study, we developed a novel chip system to easily supply a fluorescence dye at appropriate densities. We observed CNTs in solution, in real time, using fluorescence as background. Next, we trapped CNTs in ITO electrode gaps with DEP force. Finally, we clearly observed CNT samples trapped in the solution under an optical microscope. These results show that we can trap CNTs and observe them more clearly by the quenching observation method. This longtime observation

Authorized licensed use limited to: TOHOKU UNIVERSITY. Downloaded on March 10,2010 at 00:14:00 EST from IEEE Xplore. Restrictions apply.

system for CNTs will lead to major progress in nanodevices for biotechnology.

In the future, we intend to control the flow velocity or flow volume while measuring the fluorescent reagent density in real time. The density can be measured from the fluorescence microscope images. It is possible to control the flow volume of the syringe pump in real time or to place an active microvalve in the chip for providing feedback control.

REFERENCES

[1] R. H. Baughman, A. A. Zakhidov, and W. A. de Heer, "Carbon nanotubes—The route toward applications," *Science*, vol. 297, pp. 787–792, 2002.

[2] T. Fukuda, F. Arai, and L. Dong, "Assembly of nanodevices with carbon nanotubes through nanorobotic manipulations," *Proc. IEEE*, vol. 91, no. 11, pp. 1803–1818, Nov. 2003.

[3] M. Nakajima, F. Arai, and T. Fukuda, "In situ measurement of Young's modulus of carbon nanotube inside TEM through hybrid nanorobotic manipulation system," *IEEE Trans. Nanotechnol.*, vol. 5, no. 3, pp. 243–248, May 2006.

[4] J. Chen, M. A. Hamon, H. Hu, Y. Chen, A. M. Rao, P. C. Eklund, and R. C. Haddon, "Solution properties of single-walled carbon nanotubes," *Science*, vol. 282, pp. 95–98, 1998.

[5] V. Krstic, G. S. Duesberg, J. Muster, M. Burghard, and S. Roth, "Langmuir–Blodgett films of matrix-diluted single-walled carbon nanotubes," *Chem. Mater.*, vol. 10, pp. 2338–2340, 1998.

[6] K. Otobe, H. Nakao, H. Hayashi, F. Nihey, M. Yudasaka, and S. Iijima, "Fluorescence visualization of carbon nanotubes by modification with silicon-based polymer," *Nano Lett.*, vol. 2, pp. 1157–1160, 2002.

[7] S. K. Doorn, L. Zheng, M. J. O'Connell, Y. Zhu, S. Huang, and J. Liu, "Raman spectroscopy and imaging of ultralong carbon nanotubes," *Phys. Chem. B*, vol. 109, pp. 3751–3758, 2005.

[8] S. K. Doorn, M. J. O'Connell, L. Zheng, Y. Zhu, S. Huang, and J. Liu, "Raman spectral imaging of a carbon nanotube intramolecular junction," *Phys. Rev. Lett.*, vol. 94, p. 016802, 2005.

[9] K. Kaminska, J. Lefebvre, D. G. Austing, and P. Finnie, "Real-time global Raman imaging and optical manipulation of suspended carbon nanotubes," *Phys. Rev. B*, vol. 73, p. 235410, 2006.

[10] D. A. Tsyboulski, S. M. Bachilo, and R. B. Weisman, "Versatile visualization of individual single-walled carbon nanotubes with near-infrared fluorescence microscopy," *Nano Lett.*, vol. 5, pp. 975–979, 2005.

[11] L. Cognet, D. A. Tsyboulski, J.-D. R. Rocha, C. D. Doyle, J. M. Tour, and R. B. Weisman, "Stepwise quenching of exciton fluorescence in carbon nanotubes by single-molecule reactions," *Science*, vol. 316, pp. 1465–1468, 2007.

[12] H. Jin, D. A. Heller, and M. S. Strano, "Single-particle tracking of endocytosis and exocytosis of single-walled carbon nanotubes in NIH-3T3 cells," *Nano Lett.*, vol. 8, pp. 1577–1585, 2008.

[13] Z. Liu, C. Davis, W. Cai, L. He, X. Chen, and H. Dai, "Circulation and long-term fate of functionalized, biocompatible single-walled carbon nanotubes in mice probed by Raman spectroscopy," *Proc. Nat. Acad. Sci. USA*, vol. 105, pp. 1410–1415, 2008.

[14] S. Tan, H. A. Lopez, C. W. Cai, and Y. Zhang, "Optical trapping of single-walled carbon nanotubes," *Nano Lett.*, vol. 4, pp. 1415–1419, 2004.

[15] F. Arai, M. Nagai, A. Shimizu, A. Ishijima, and T. Fukuda, "Fluorescence visualization of carbon nanotubes using quenching effect for nanomanipulation," in *Proc. IEEE-NEMS*, Bangkok, Thailand, 2007, pp. 312–315.

[16] A. Vijayaraghavan, S. Blatt, D. Weissenberger, M. Oron-Carl, F. Hennrich, D. Gerthsen, H. Hahn, and R. Krupke, "Ultra-large-scale directed assembly of single-walled carbon nanotube devices," *Nano Lett.*, vol. 7, pp. 1556–1560, 2007.

[17] S. Blatt, F. Hennrich, H. v. Löhneysen, M. M. Kappes, A. Vijayaraghavan, and R. Krupke, "Influence of structural and dielectric anisotropy on the dielectrophoresis of single-walled carbon nanotubes," *Nano Lett.*, vol. 7, pp. 1960–1966, 2007.

[18] L. Dong, B. J. Nelson, T. Fukuda, and F. Arai, "Towards nanotube linear servomotors," *IEEE Trans. Autom. Sci. Eng.*, vol. 3, no. 3, pp. 228–235, Jul. 2006.

[19] A. Subramanian, L. Dong, J. Tharian, U. Sennhauser, and B. J. Nelson, "Batch fabrication of carbon nanotube bearings," *Nanotechnology*, vol. 18, pp. 075703-1–075703-9, 2007.

[20] W. C. Jackson, H. D. Tran, M. J. O'Brien, E. Rabinovich, and G. P. Lopez, "Rapid prototyping of active microfluidic components based on magnetically modified elastomeric materials," *J. Vac. Sci. Technol. B*, vol. 19, pp. 596–599, 2001.

[21] D. Olivier, T. Abdelkrim, D. Yves, G. Leticia, T. Nicolas, P. Philippe, P. Vladimir, and M. Alain, "Magnetically actuated microvalve for active flow control," *J. Phys.: Conf. Ser.*, vol. 34, pp. 631–636, 2006.

[22] Y. Yamanishi, Y.-C. Lin, and F. Arai, "Magnetically modified PDMS devices for micro particle manipulation," in *Proc. IEEE Int. Conf. Intell. Robot. Syst.*, San Diego, CA, 2007, pp. 753–758.

[23] J. Zhang, J. Tang, G. Yang, Q. Qiu, L. C. Qin, and O. Zhou, "Efficient fabrication of carbon nanotube point electron sources by dielectrophoresis," *Adv. Mater.*, vol. 16, pp. 1219–1222, 2004.

[24] W. L. Murphy, R. G. Dennis, J. L. Kileny, and D. J. Mooney, "Salt fusion: An approach to improve pore interconnectivity within tissue engineering scaffolds," *Tissue Eng.*, vol. 8, no. 1, pp. 43–52, 2002.

[25] N. Nakashima, Y. Tomonari, and H. Murakami, "Water-soluble single-walled carbon nanotubes via noncovalent sidewall-functionalization with a pyrene-carrying ammonium ion," *Chem. Lett.*, vol. 31, pp. 638–639, 2002.

[26] R. J. Chen, Y. Zhang, D. Wang, and H. Dai, "Noncovalent sidewall functionalization of single-walled carbon nanotubes for protein immobilization," *J. Amer. Chem. Soc.*, vol. 123, pp. 3838–3839, 2001.

Authors' photographs and biographies not available at the time of publication.

Authorized licensed use limited to: TOHOKU UNIVERSITY. Downloaded on March 10,2010 at 00:14:00 EST from IEEE Xplore. Restrictions apply.